

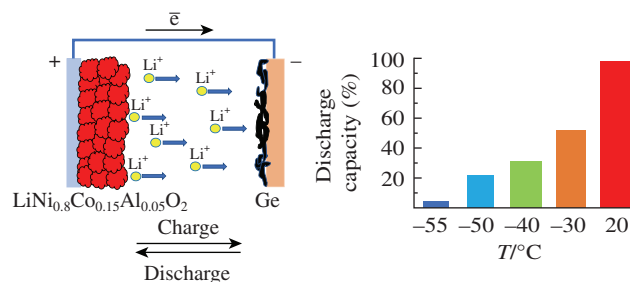
A $\text{LiNi}_{0.8}\text{Co}_{0.15}\text{Al}_{0.05}\text{O}_2/\text{Ge}$ electrochemical system for lithium-ion batteries

Tatiana L. Kulova, Ilya M. Gavrilin, Yulia O. Kudryashova and Alexander M. Skundin*

A. N. Frumkin Institute of Physical Chemistry and Electrochemistry, Russian Academy of Sciences, 119071 Moscow, Russian Federation. E-mail: askundin@mail.ru

DOI: 10.1016/j.mencom.2020.11.029

The title system with a positive electrode based on a $\text{LiNi}_{0.8}\text{Co}_{0.15}\text{Al}_{0.05}\text{O}_2$ mixed layered oxide and a negative electrode of filamentary germanium nanostructures can operate at low temperatures (to -55°C) in an electrolyte based on propylene carbonate. The energy density of such a battery is about 400 Wh kg^{-1} (in terms of active compounds), which exceeds that of commercial LiCoO_2/C batteries by a factor of 1.25.



Keywords: lithium-ion battery, germanium nanostructures, $\text{LiNi}_{0.8}\text{Co}_{0.15}\text{Al}_{0.05}\text{O}_2$, propylene carbonate–dimethoxyethane, low temperatures.

Lithium-ion batteries are most popular rechargeable power sources because of a high energy density and good cyclability.¹ Lithiated cobalt oxide (positive electrode)/graphite (negative electrode) is the most common electrochemical system in modern commercial lithium-ion batteries.² Less popular are electrochemical systems with a positive electrode based on lithium iron phosphate or a mixed layered oxide, while silicon–carbon composites or lithium titanate can be used as a negative electrode.^{3–5} As a rule, a 1 M solution of lithium hexafluorophosphate in a mixture of ethylene carbonate, diethyl carbonate and dimethyl carbonate (1 : 1 : 1) is used as an electrolyte in these batteries.⁶ All modern lithium-ion batteries lose their performance at temperatures below -20°C .

In this work, we suggest a new electrochemical system for lithium-ion batteries with a positive electrode based on the mixed layered oxide $\text{LiNi}_{0.8}\text{Co}_{0.15}\text{Al}_{0.05}\text{O}_2$, a negative electrode of filamentary germanium nanostructures and an electrolyte of 1 M LiClO_4 in a propylene carbonate–dimethoxyethane mixture (7 : 3).

Commercial $\text{LiNi}_{0.8}\text{Co}_{0.15}\text{Al}_{0.05}\text{O}_2$ from Gelon LIB (PRC) was used. Filamentary germanium nanostructures were synthesized by cathodic deposition on a titanium substrate from an aqueous solution of germanium oxides according to a procedure described previously.^{†,7} As found by scanning electron microscopy, the morphology of germanium synthesized in this way was represented by filamentary nanostructures with an average diameter of about 40 nm (Figure 1).

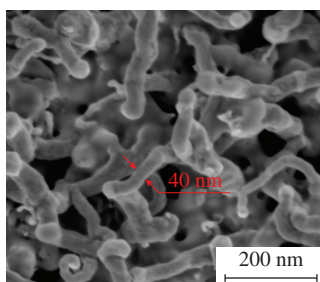


Figure 1 SEM image of germanium filamentary nanostructures.

Electrodes from $\text{LiNi}_{0.8}\text{Co}_{0.15}\text{Al}_{0.05}\text{O}_2$ were manufactured by a traditional technique.[‡] The electrochemical performances of electrodes were studied using a galvanostatic method.[§]

Galvanostatic testing of germanium electrodes at a current density of 1385 mA g^{-1} (1C) showed that the discharge capacity of germanium (during lithium deintercalation) was about 1350 mAh g^{-1} (the theoretical specific capacity of germanium is 1385 mAh g^{-1}), and it remained almost unchanged upon cycling [Figure 2(a)]. The mean potential in the course of lithium extraction from germanium was about 0.6 V. The specific capacity upon lithium insertion in the first cycle slightly exceeded the specific capacity upon lithium extraction due to an irreversible electrochemical process, *i.e.*, the reduction of the electrolyte on the surface of germanium nanowires and the formation of a solid electrolyte film (solid electrolyte interface).^{8,9}

The charge–discharge curves of $\text{LiNi}_{0.8}\text{Co}_{0.1}\text{Al}_{0.05}\text{O}_2$ in Figure 2(b) show that, at a current density of 290 mA g^{-1} (1C), the discharge capacity (when lithium was inserted into $\text{LiNi}_{0.8}\text{Co}_{0.1}\text{Al}_{0.05}\text{O}_2$) was about 180 mAh g^{-1} , and it was stable in the course of cycling. The average discharge potential of

[†] The deposition current density was 2 mA cm^{-2} , and the amount of the active electrode material was about 0.12 mg cm^{-2} .

[‡] To prepare the electrodes, a cathode slurry consisting of 85% $\text{LiNi}_{0.8}\text{Co}_{0.15}\text{Al}_{0.05}\text{O}_2$, 10% carbon black and 5% polyvinylidene fluoride dissolved in *N*-methylpyrrolidone was applied onto an aluminum foil substrate, dried to constant weight, compressed at 2 t cm^{-2} and then dried *in vacuo* to remove water traces. The amount of $\text{LiNi}_{0.8}\text{Co}_{0.15}\text{Al}_{0.05}\text{O}_2$ on the electrode was $\sim 2\text{ mg cm}^{-2}$.

[§] To determine the electrochemical characteristics, three-electrode cells were assembled of a working electrode ($\text{LiNi}_{0.8}\text{Co}_{0.15}\text{Al}_{0.05}\text{O}_2$ or Ge), a lithium auxiliary electrode and a lithium reference electrode. Laboratory cells had a prismatic design and contained $3 \times 4\text{ cm}^2$ electrodes. Laminated aluminum foil 150 μm thick was used as a battery case, which was sealed using a Henkelman Mini Jumbo vacuum sealer. The water content of the electrolyte measured by K. Fischer coulometric titration (917 Ti-Touch, Metrohm, Switzerland) did not exceed 15 ppm. Electrochemical cells and battery models were assembled in an airtight glove box (Spectroscopic Systems, Russia) containing no more than 1 ppm water and oxygen.

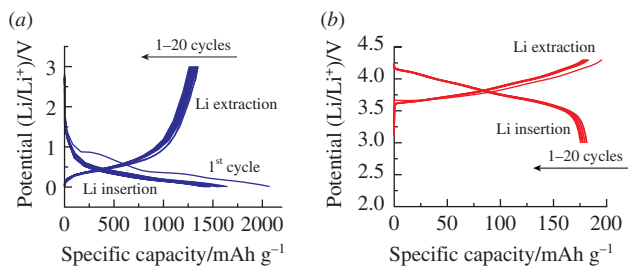


Figure 2 Charge–discharge curves of electrodes made of (a) filamentary germanium nanostructures and (b) $\text{LiNi}_{0.8}\text{Co}_{0.15}\text{Al}_{0.05}\text{O}_2$ at a current of 1C.

$\text{LiNi}_{0.8}\text{Co}_{0.15}\text{Al}_{0.05}\text{O}_2$ was about 3.8 V. In general, the charge and discharge curves on a $\text{LiNi}_{0.8}\text{Co}_{0.15}\text{Al}_{0.05}\text{O}_2$ electrode are consistent with published data.^{10,11}

Taking into consideration the experimental specific discharge capacities of the electrodes based on filamentary germanium nanostructures and $\text{LiNi}_{0.8}\text{Co}_{0.15}\text{Al}_{0.05}\text{O}_2$ and the irreversible capacity of germanium electrodes at the first cycle, we calculated the weights of $\text{LiNi}_{0.8}\text{Co}_{0.15}\text{Al}_{0.05}\text{O}_2$ and germanium in the electrodes for the full cell using the following relationship:

$$\frac{Q_c^d}{Q_a^d + Q_a^{\text{ir}}} = \frac{m_a}{m_c}, \quad (1)$$

where Q_c^d is the discharge capacity of the $\text{LiNi}_{0.8}\text{Co}_{0.15}\text{Al}_{0.05}\text{O}_2$ cathode, Q_a^d is the discharge capacity of the germanium anode, Q_a^{ir} is the irreversible capacity of the anode, m_a is the weight of the anode active material, and m_c is the weight of the cathode active material. Thus, for the anodes with a germanium sample of 0.12 mg cm^{-2} , the amount of $\text{LiNi}_{0.8}\text{Co}_{0.15}\text{Al}_{0.05}\text{O}_2$ on the positive electrodes was about 1.13 mg cm^{-2} . The full cells of the $\text{LiNi}_{0.8}\text{Co}_{0.15}\text{Al}_{0.05}\text{O}_2/\text{Ge}$ system were tested at a current of 1C and at various temperatures. Figure 3(a) shows a stable battery cycling (the charging and discharging curves of 25 cycles) with an average voltage of $\sim 3 \text{ V}$ and a capacity of $\sim 2 \text{ mAh}$. The capacity and discharge voltage of the battery decreased with decreasing the operating temperature [Figure 3(b)]. At temperatures of -20 , -30 , -40 , -50 and -55°C , the discharge capacities were 1.34, 1.06, 0.64, 0.42 and 0.11 mAh , respectively.

Figure 4 (in Arrhenius coordinates^{12,13}) clearly shows how the capacity of a new battery changes with temperature. In general, the plot shown in Figure 3 is also characteristic of batteries belonging to other electrochemical systems, for example, laboratory model batteries of the $\text{LiNi}_{0.8}\text{Co}_{0.15}\text{Al}_{0.05}\text{O}_2/\text{graphite}$ system with various electrolytes¹⁴ and commercial lithium–polymer batteries.¹⁵

Thus, the advantage of the $\text{LiNi}_{0.8}\text{Co}_{0.15}\text{Al}_{0.05}\text{O}_2/\text{Ge}$ lithium-ion battery over a commercial LiCoO_2/C battery is that it has a higher energy density and can operate at lower temperatures.

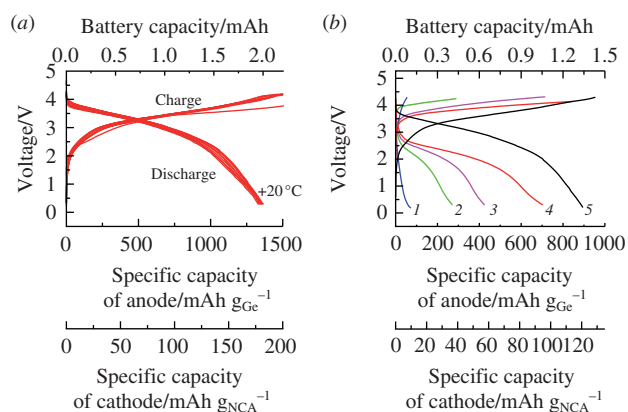


Figure 3 Charge–discharge curves of a $\text{LiNi}_{0.8}\text{Co}_{0.15}\text{Al}_{0.05}\text{O}_2/\text{Ge}$ full cell at a discharge current of 1C (a) at room temperature and (b) at different low temperatures ($^\circ\text{C}$): (1) -55 , (2) -50 , (3) -40 , (4) -30 , (5) -20 .

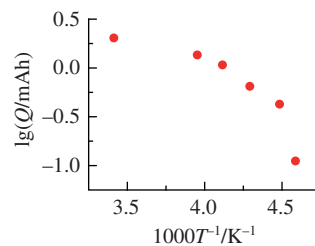


Figure 4 The temperature dependence of the capacity of a $\text{LiNi}_{0.8}\text{Co}_{0.15}\text{Al}_{0.05}\text{O}_2/\text{Ge}$ full cell.

The energy density of a $\text{LiNi}_{0.8}\text{Co}_{0.15}\text{Al}_{0.05}\text{O}_2/\text{Ge}$ battery at a current of 1C was 400 Wh kg^{-1} with respect to the weight of the active materials. The energy density of a commercial LiCoO_2/C battery at a current of 1C in terms of the active compounds is about 320 Wh kg^{-1} . The ability of the $\text{LiNi}_{0.8}\text{Co}_{0.15}\text{Al}_{0.05}\text{O}_2/\text{Ge}$ battery to operate at lower temperatures is due to the electrolyte based on a propylene carbonate–DME mixture (with a freezing temperature of -70°C), which can be used in combination with a germanium electrode but not with carbon electrodes. Carbon-based electrodes do not provide stable cycling in propylene carbonate-based electrolytes due to a large fraction of irreversible processes of propylene carbonate reduction on the carbon surface.^{16,17}

This work was supported by the Ministry of Science and Higher Education of the Russian Federation.

References

- A. B. Yaroslavtsev, I. A. Stenina, T. L. Kulova, A. M. Skundin and A. V. Desyatov, in *Comprehensive Nanoscience and Nanotechnology*, 2nd edn., eds. D. Andrews, T. Nann and R. Lipson, Elsevier, Academic Press, 2019, vol 5, pp. 165–206.
- C. Julien, A. Mauger, A. Vijn and K. Zaghib, *Lithium Batteries: Science and Technology*, Springer, 2016.
- A. B. Yaroslavtsev, T. L. Kulova and A. M. Skundin, *Russ. Chem. Rev.*, 2015, **84**, 826.
- N. Nitta, F. Wu, J. T. Lee and G. Yushin, *Mater. Today*, 2015, **18**, 252.
- W.-J. Zhang, *J. Power Sources*, 2011, **196**, 2962.
- R. W. Schmitz, P. Murmann, R. Schmitz, R. Müller, L. Krämer, J. Kasnatscheew, P. Isken, P. Niehoff, S. Nowak, G.-V. Rösenthaler, N. Ignatiev, P. Sartori, S. Passerini, M. Kunze, A. Lex-Balducci, C. Schreiner, I. Cekic-Laskovic and M. Winter, *Prog. Solid State Chem.*, 2014, **42**, 65.
- I. M. Gavrilin, V. A. Smolyaninov, A. A. Dronov, S. A. Gavrilov, A. Yu. Trifonov, T. L. Kulova, A. A. Kuz'mina and A. M. Skundin, *Mendeleev Commun.*, 2018, **28**, 659.
- L. Ma, E. Fahrenkrug, E. Gerber, A. J. Crowe, F. Venable, B. M. Bartlett and S. Maldonado, *ACS Energy Lett.*, 2017, **2**, 238.
- J. Graetz, C. C. Ahn, R. Yazami and B. Fultz, *J. Electrochem. Soc.*, 2004, **151**, A698.
- K. Kimura, T. Sakamoto, T. Mukai, Y. Ikeuchi, N. Yamashita, K. Onishi, K. Asami and M. Yanagida, *J. Electrochem. Soc.*, 2018, **165**, A16.
- M. Liang, Y. Sun, D. Song, X. Shi, Y. Han, H. Zhang and L. Zhang, *Electrochim. Acta*, 2019, **300**, 426.
- T. L. Kulova, *Russ. J. Electrochem.*, 2004, **40**, 1052 (*Elektrokhimiya*, 2004, **40**, 1221).
- E. K. Tuseeva, T. L. Kulova and A. M. Skundin, *Russ. J. Electrochem.*, 2018, **54**, 1186 (*Elektrokhimiya*, 2018, **54**, 1135).
- Q. Li, S. Jiao, L. Luo, M. S. Ding, J. Zheng, S. S. Cartmell, C.-M. Wang, K. Xu, J.-G. Zhang and W. Xu, *ACS Appl. Mater. Interfaces*, 2017, **9**, 18826.
- A. M. Aris and B. Shabani, *Energy Procedia*, 2017, **110**, 128.
- Lithium Batteries: Science and Technology*, eds. G. A. Nazri and G. Pistoia, Springer, 2009.
- D. Aurbach, B. Markovsky, I. Weissman, E. Levi and Y. Ein-Eli, *Electrochim. Acta*, 1999, **45**, 67.

Received: 30th April 2020; Com. 20/6212